THE JOURNAL OF PHYSICAL CHEMISTRY B

Article

pubs.acs.org/JPCB

Quasi-Chemical Theory of Cosolvent Hydrophobic Preferential Interactions

M. Hamsa Priya,[†] Safir Merchant,[‡] Dilip Asthagiri,[‡] and Michael E. Paulaitis*,[†]

[†]William G. Lowrie Department of Chemical and Biomolecular Engineering, The Ohio State University, Columbus, Ohio 43210, United States

[‡]Department of Chemical and Biomolecular Engineering, Johns Hopkins University, Baltimore, Maryland 21218, United States

Supporting Information

ABSTRACT: Cosolvent hydrophobic preferential interactions with methane in aqueous methanol solutions are evaluated on the basis of the solute excess chemical potential derived from molecular simulations using the quasi-chemical (QC) theory generalization of the potential distribution theorem (PDT). We find that the methane–methanol preferential interaction parameter derived from QC theory quantitatively captures the favorable solvation of methane in methanol solutions in terms of important local solute–solvent (water and methanol) intermolecular interactions within a defined inner shell around the solute, and nonlocal solute interactions with solvent molecules outside this inner shell. Moreover, a unique inner shell can be defined such that the preferential interaction parameter is derived exclusively from the free energy of cavity formation in the aqueous cosolvent solution without the solute, where this cavity corresponds to the specified inner shell, and the mean interaction or binding energy of the solute with solvent molecules outside this inner shell. This inner-shell definition leads to a description of solute–cosolvent preferential interactions in which the molecular details of those interactions are derived from the effect of cosolvent on cavity statistics in the aqueous cosolvent solution alone. The finding suggests that solution thermodynamic behavior beyond steric exclusion (macromolecular crowding) contribute to the molecular mechanisms by which cosolvent preferential interactions influence protein stability and activity.

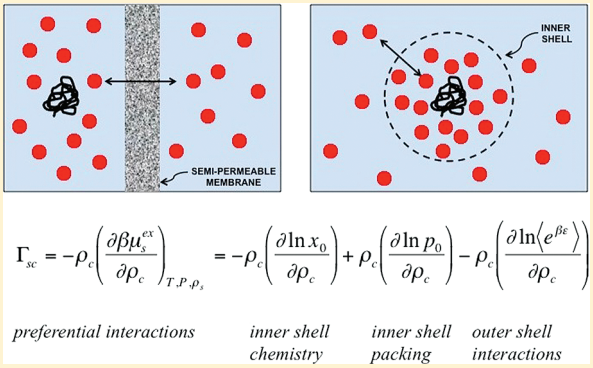

I. INTRODUCTION

Cosolvent effects on the hydration of biological macromolecules arise naturally in describing thermodynamic driving forces for molecular recognition and self-assembly. These effects take on added significance when the solute is a chemically heterogeneous macromolecule, since the cosolvent can interact directly with specific, solvent-accessible sites on the solute, as well as indirectly influence the hydration of other sites. This indirect influence on hydration becomes especially important when the solute is a protein, since hydration and the ability to impact hydration with cosolvents can play a central role in the configurational stability of proteins, their self-assembly into functional molecules or molecular complexes, and ligand binding,[1−5] as well as protein phase behavior, e.g., protein crystallization,[6,7] aggregation,[8,9] adsorption,[10,11] and fibril formation.[12−14]

For nonionic, amphiphilic cosolvents, such as monohydric alcohols or polyols, hydrophobic preferential interactions between methyl groups of the cosolvent and hydrophobic regions on the protein surface can effectively compete with protein adsorption at hydrophobic interfaces to inhibit aggregation and the partial or complete unfolding of the protein. This competitive mechanism has also been invoked to explain how cosolvents, such as glycerol, can inhibit weak protein–protein attractions that lead to protein aggregation in aqueous solution.[1,15−19]

Local hydrophobic preferential interactions between amphiphilic cosolvents and sites on a protein surface will, however, be sensitive to the local topography and chemical composition of the protein surface. Consequently, more stringent demands are placed on the spatial resolution of cosolvent preferential interactions computed across such surfaces. Molecular simulations can supply detailed descriptions of local water and cosolvent densities at specific solvent-accessible sites on the surface of a protein relative to bulk solution densities, but converting this information into a quantitative measure of site-specific preferential interactions lacks high spatial resolution.[20−23]

An entirely different analysis of molecular simulations is presented here that does not rely on solute–water and solute–cosolvent molecular distribution functions. Instead, preferential interactions are evaluated directly from the solute excess

Received: February 18, 2012
Revised: May 6, 2012
Published: May 9, 2012

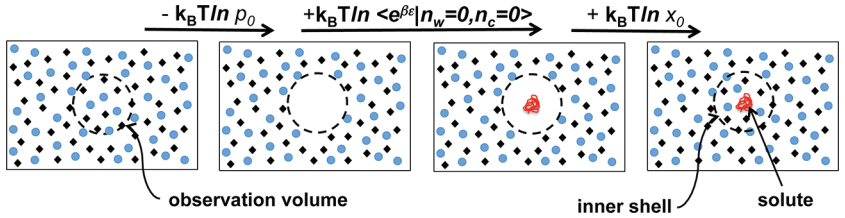

Figure 1. Solvation of a solute in an aqueous cosolvent solution. The dashed circles represent an observation volume in the aqueous solution without the solute and the inner shell around the solute in the aqueous solution containing the solute. Cosolvent molecules are represented by black diamonds, water by the blue circles, and the solute molecule as a compact, red chain. The occupancy probabilities, x_0 and p_0, are, respectively, the probabilities of finding no solvent (water and cosolvent) molecules in the defined inner shell with and without the solute present, $-k_BT \ln p_0 > 0$ is the free energy of creating a cavity in solution the size and shape of the inner shell, $+k_BT \ln x_0 < 0$ is the free energy of forming clusters of cosolvent and water molecules with the solute in the inner shell, and $+k_BT \ln\langle e^{\beta\varepsilon}|n_w = n_c = 0\rangle < 0$ is the interaction free energy of inserting the solute molecule in the empty inner shell.

chemical potential, derived from molecular simulations using the potential distribution theorem (PDT) and quasi-chemical (QC) theory.[24−26] The QC generalization of the PDT has been applied successfully to evaluate hydration free energies for a variety of solutes, including hydrophobic solutes at infinite dilution in water.[27−29] We extend this QC/PDT approach to hydrophobic solutes in aqueous cosolvent solutions by considering methanol (cosolvent) preferential interactions with methane in aqueous methanol solutions. We show that a unique inner-shell volume can be identified for which methane−methanol preferential interactions are described exclusively in terms of the free energy of cavity formation in the aqueous methanol solution alone, and the mean interaction or binding energy of methane with water and methanol molecules outside an inner shell around the solute defined by this cavity. Since this inner shell includes only a fraction of the first solvation shell of the solute, higher spatial resolution can be achieved in evaluating cosolvent preferential interactions with more complex molecular solutes.

II. QUASI-CHEMICAL DESCRIPTION OF PREFERENTIAL INTERACTIONS

Our evaluation of solute−cosolvent preferential interactions focuses on the excess chemical potential of the solute, μ_s^{ex}, which accounts for solute interactions with the cosolvent and water molecules through $P(\varepsilon)$, the probability distribution of solute−solvent interaction or binding energies, ε, given by the PDT,[30,31]

$$e^{\beta\mu_s^{ex}} = \int P(\varepsilon)e^{+\beta\varepsilon}\, d\varepsilon = \langle e^{+\beta\varepsilon}\rangle \tag{1}$$

The binding energy for a particular configuration is the difference in the potential energy of the entire solution (solute and solvent) and the sum of the potential energies of the solute and the solvent as separate subsystems. Evaluation of the binding energy does not require pairwise decomposable intermolecular interactions. The brackets following the right-most equality represent thermal averaging over all the possible solute−solvent configurations with the solute fully coupled to the solvent at temperature $T = 1/k_B\beta$, with k_B Boltzmann's constant.

Solute−solvent intermolecular interactions in QC theory are partitioned into local interactions within a defined local domain or inner shell around the solute and nonlocal solute interactions with solvent molecules outside this inner shell. This partitioning leads to the formal identity,[24−26]

$$\beta\mu_s^{ex} = \ln x_0/p_0 + \ln\langle e^{\beta\varepsilon}|n_w = 0, n_c = 0\rangle \tag{2}$$

where n_i is the number of molecules of each component i = s, w, and c for the solute, water, and cosolvent, respectively. Figure 1 provides a physical interpretation of each term in this expression. The occupancy probability, x_0, is the probability that the defined inner shell around the solute contains no solvent molecules, while the occupancy probability, p_0, is the probability of finding a cavity in the aqueous cosolvent solution that has the size and shape of the defined inner shell. The free energy of binding the solute with solvent in the outer shell under the condition that no solvent molecules occupy the inner shell is given by $\ln\langle e^{\beta\varepsilon}|n_w = 0, n_c = 0\rangle$. If the corresponding conditional probability distribution of solute binding energies is accurately Gaussian, then this free energy is given by the mean and the variance of that distribution,[28,29,32,33] and

$$\beta\mu_s^{ex} = \ln x_0 - \ln p_0 + \beta\langle\varepsilon\rangle + \beta^2\sigma^2/2 \tag{3}$$

To simplify notation, we omit designations of the condition that $n_w = 0$ and $n_c = 0$ on the mean binding energy, $\langle\varepsilon\rangle$, and the variance, σ^2, in this expression and from here on. Following Timasheff,[1] solute−cosolvent preferential interactions are defined as the extent to which adding cosolvent to an aqueous solution containing the solute perturbs the solute chemical potential. This perturbation is expressed by the preferential interaction parameter

$$\Gamma_{sc} = -\rho_c\left(\frac{\partial\beta\mu_s^{ex}}{\partial\rho_c}\right)_{T,P,\rho_s} \tag{4}$$

Adding cosolvent increases solute solubility when $\Gamma_{sc} > 0$ (salting in), and conversely, reduces solute solubility when $\Gamma_{sc} < 0$ (salting out). The preferential interaction parameter expressed in terms of the QC contributions to μ_s^{ex} is

$$\Gamma_{sc} = -\rho_c\left(\frac{\partial \ln x_0}{\partial\rho_c}\right)_{T,P,\rho_s} + \rho_c\left(\frac{\partial \ln p_0}{\partial\rho_c}\right)_{T,P,\rho_s} - \rho_c\left(\frac{\partial \ln\langle e^{\beta\varepsilon}\rangle}{\partial\rho_c}\right)_{T,P,\rho_s} \tag{5}$$

The inner-shell contribution is given by the first two terms on the right side of this expression, and can be viewed as the effect of cosolvent on the intrinsic propensity of the solvent to occupy an inner-shell volume in solution with and without the solute present.[34] Nonlocal solute interactions with the outer-shell

dx.doi.org/10.1021/jp301629j | J. Phys. Chem. B 2012, 116, 6506−6513

solvent also contribute through the cosolvent concentration dependence of the binding free energy of the solute with solvent in the outer shell, the rightmost term in eq 5. This contribution accounts for the stabilization of solute−solvent molecular clusters in the inner shell by the outer-shell solvent.[35] Thus, certain solvent molecular clusters will be preferentially stabilized over others depending on the bulk concentration of cosolvent.

In contrast to the QC description of preferential interactions, the Kirkwood-Buff (KB) theory description differentiates the local domain around a solute from bulk solution based on differences in the solvent composition that arise as a consequence of the preferential partitioning of water or cosolvent molecules in the local domain. The KB preferential interaction parameter expresses these differences in terms of cosolvent and water molecular distributions around the solute[36,37]

$$\Gamma_{sc} = \rho_c(G_{sc} - G_{sw}) \tag{6}$$

where the KB integrals,

$$G_{si}(R) \approx 4\pi \int_0^R (g_{si}(r) - 1)r^2 \, dr \tag{7}$$

are estimated from cosolvent−solute and water−solute radial distribution functions within a local domain around the solute that, in practice, is taken to be a subsystem within a much larger, closed simulation system.[38−41] This local domain in eq 7 is defined as a sphere of radius, R, centered on the solute, and the radial distribution function, $g_{si}(r)$, is evaluated from $\rho_i(r < R) \equiv \rho_i g_{si}(r < R)$, the density of component i (= c or w) within the local domain. The bulk solution density, ρ_i, required for the normalization of $g_{si}(r)$ is evaluated in the limit of $g_{si}(r > R) \to 1$, which defines R as the radial distance beyond which $g_{si}(r > R) = 1$.

Although long-range oscillations intrinsic to the KB integrals can be suppressed by spatially "smearing" the distribution functions,[42−45] even small deviations from $g_{si}(r > R) \to 1$ can lead to the divergence of Γ_{sc} with increasing R in the bulk solution limit.[45] By taking advantage of intermolecular interactions instead of longer range intermolecular positional correlations to distinguish local from nonlocal solute−solvent interactions, the QC/PDT approach avoids this problem of the divergence of Γ_{sc} in the bulk solution limit. Moreover, in explicitly providing molecular details of the relationship between local solute−solvent intermolecular interactions and the solute excess chemical potential, the QC/PDT approach offers insights into preferential molecular interactions that cannot be obtained by considering molecular radial distribution functions alone.

III. SIMULATION DETAILS

All simulations were carried out using NAMD 2.6[46] with an integration time step of 2 fs. The numbers of water and methanol molecules in each simulation system are given in Table 1. United atom OPLS models[47,48] were used for methane and methanol, and the TIP3P model was used for water.[49]

Each system was initially relaxed by executing 10 000 steps of conjugate gradient energy minimization, and then equilibrated for 3 ns at 300 K and 1 bar. The simulation box size was then fixed to the average box size for the final 2 ns of this constant NPT simulation, and the system further equilibrated for 1 ns at constant volume and 300 K. Configurations were saved every 0.1 ps over a 25 ns constant NVT production run.

Table 1. Number of Methanol and Water Molecules in the Simulation System as a Function of Methanol Composition

methanol mole fraction	methanol	water
0.00	0	4096/1728[a]
0.05	205	3891
0.10	410	3686
0.20	820	3276
0.30	1229	2867
1.00	4096	0

[a]The first number refers to methane in water; the second number refers to pure water.

Temperature was held constant by applying Langevin dynamics to all heavy atoms using a damping coefficient of 1 ps^{-1}. Constant pressure was maintained using a Nosé−Hoover Langevin piston[50,51] with a period of 200 fs and a decay of 100 fs. Periodic boundary conditions were imposed, and the particle-mesh Ewald method[52] with a real-space cutoff of 12 Å was applied in computing the electrostatic interactions. The nonbonded dispersion interactions were smoothly switched to zero at 12 Å starting from 10 Å. The SHAKE algorithm[53] was used to constrain the positions of all hydrogen atoms.

The cavity probability, p_0, at each solvent composition given in Table 1 was obtained directly from the simulations by placing a cubic grid in the simulation box, and finding the fraction of solvent configurations for which no water oxygen centers were located within a radial distance of λ_w around each grid point, and no methanol methyl and hydroxyl group centers were located within radial distances of λ_w + 0.3 Å and λ_w + 0.6 Å, respectively, around each grid point. Spacing between the grid points was 2 Å. The inner-shell occupancy probability, x_0, at each solvent composition was obtained by applying the same procedure to a single grid point defined by the center of the methane molecule.

IV. RESULTS AND DISCUSSION

The inner shell for water molecules around methane is defined to be a sphere centered on methane with radius λ_w = 3.3 Å. This radius corresponds to the distance at which the water oxygen−methane radial distribution functions (rdfs) in Figure 2 first equal unity, and is insensitive to methanol concentration. The inner shell for methanol molecules is defined by two radii,[54] λ_m = 3.6 Å for the methyl group and λ_h = 3.9 Å for the hydroxyl group of methanol. These radii likewise correspond to distances at which the methyl group−methane and hydroxyl group−methane rdfs in Figure 3 first equal unity, and are insensitive to methanol concentration. We note that the primary peaks for the methyl group−methane rdfs are higher, narrower, and closer to methane compared to those for the hydroxyl group−methane rdfs, indicating that the near-neighbor methanol molecules are oriented with their methyl groups pointing toward methane, as expected for hydrophobic interactions between the two molecules.

Figure 4 shows the binding energy probability distributions for methane with water and methanol in the two pure solvents under the condition that no solvent molecules occupy the inner shell around the solute. This conditioning gives a nearly Gaussian distribution in both cases by eliminating close-contact repulsive interactions with methane that contribute to the important high-energy tails of the probability distributions.

dx.doi.org/10.1021/jp301629j | J. Phys. Chem. B 2012, 116, 6506−6513

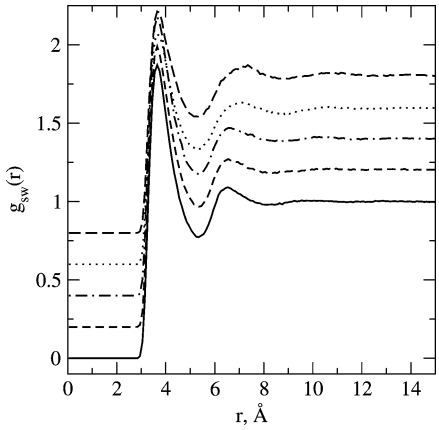

Figure 2. Radial distribution functions (rdfs) for water oxygens around a methane molecule in water (solid line) and in aqueous methanol solutions at methanol mole fractions of 0.05 (dashed line), 0.10 (dash-dotted line), 0.20 (dotted line), and 0.30 (long dashed line). Rdfs are shifted successively upward by 0.2 units for clarity.

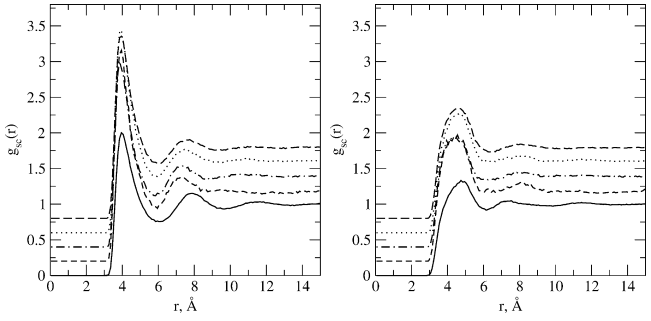

Figure 3. Radial distribution functions (rdfs) for methanol methyl groups (left) and hydroxyl groups (right) around a methane molecule in methanol (solid line) and in aqueous methanol solutions at methanol mole fractions of 0.05 (dashed line), 0.10 (dash-dotted line), 0.20 (dotted line), and 0.30 (long dashed line). Rdfs are shifted successively upward by 0.2 units for clarity.

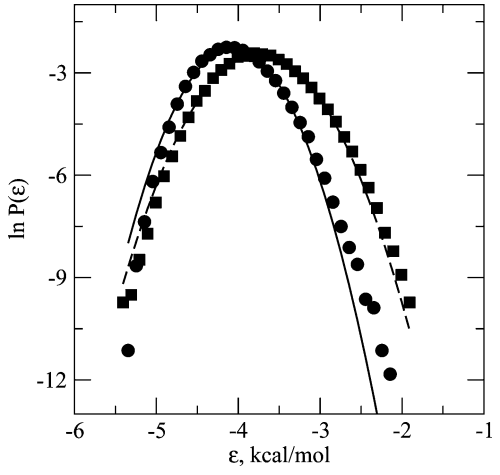

Figure 4. Conditional probability distributions of binding energies for methane in water (circles) and in methanol (squares) when no water oxygens are within λ_w = 3.3 Å of methane in water and no methanol methyl and hydroxyl groups are within λ_m = 3.6 Å and λ_h = 3.9 Å, respectively, of methane in methanol. Lines are Gaussian fits to the data.

Larger deviations from Gaussian behavior are observed in the high-energy tail of the distribution for methane in water. Nonetheless, the estimated error in μ_s^{ex} introduced by the Gaussian approximation is on the order of only 10^{-2} kcal/mol,[33] which is comparable to the statistical uncertainty in sampling the binding energies. See the table and associated text in the Supporting Information.

The individual QC contributions to μ_s^{ex} and the resulting μ_s^{ex} are plotted in Figure 5 as a function of the inner-shell radii for methane in water and in methanol. In both cases, μ_s^{ex} is independent of the inner-shell definition, as expected. However, the free energies of cavity formation and chemical association are sensitive to the inner-shell definition. More work is required to create larger cavities in either solvent, while the formation of solute−solvent molecular clusters becomes more favorable as the inner shell grows in size to include more ligand molecules. The two contributions compensate one another such that their net contribution to μ_s^{ex} is insensitive to the definition of the inner shell. The net outer-shell contribution to μ_s^{ex} from the mean binding energy and the binding-energy fluctuation contribution are likewise insensitive to the defined inner shell. The magnitude of the fluctuation contribution is also negligible in both cases. Thus, the dominant outer-shell contribution to μ_s^{ex} is the favorable mean binding energy. As expected, the greatest distinction between μ_s^{ex} for methane in the two pure solvents can be attributed to the free energy of cavity formation, $-k_BT \ln p_0$ (eq 2).[55,56]

The methanol concentration dependence of each QC contribution to μ_s^{ex} is given in Table 2. Since a species-dependent definition of the inner shell is used for the aqueous methanol solutions, we cannot compare the cavity formation and chemical association free energy contributions for methane in pure water with those for methane in aqueous solution at finite methanol concentrations. With this caveat in mind, we find that the unfavorable free energy of cavity formation dominates at all methanol concentrations. This free energy is offset in large part by the favorable mean binding energy of the solute with the outer-shell solvent. Free energy contributions from chemical association and the binding energy fluctuations are an order of magnitude smaller and partially offset one another. Independent calculations of μ_s^{ex} using histogram overlap[25,26,57] are also in excellent agreement with the QC-derived μ_s^{ex} over the entire range of methanol concentrations.

The hydration free energy of methane in Table 2 calculated using the Gaussian model (eq 3) is slightly less than μ_s^{ex} = 2.23 kcal/mol obtained by thermodynamic integration of simulation trajectories for united-atom OPLS methane in TIP3P water.[58] The difference is attributed to the shorter cutoff distance used to truncate nonbonded dispersion interactions between methane and water in computing the free energy by thermodynamic integration. Both free energies are marginally higher than the range of measured hydration free energies: 1.94−2.01 kcal/mol.[59−61] The calculated free energy of methane solvation in methanol is in excellent agreement with the measured value of 0.39 kcal/mol.[59]

The ρ_c-dependence of each QC contribution to μ_s^{ex} is also plotted in Figure 6. In each case, the dependence is linear up to a methanol mole fraction of 0.30. The negative ρ_c-dependence of μ_s^{ex} tracks closely with those for the free energies of cavity formation and chemical association. In contrast, the mean binding energy becomes slightly less negative with increasing methanol concentration. The ρ_c-dependence of the binding energy fluctuation contribution is negligible in comparison.

dx.doi.org/10.1021/jp301629j | J. Phys. Chem. B 2012, 116, 6506−6513

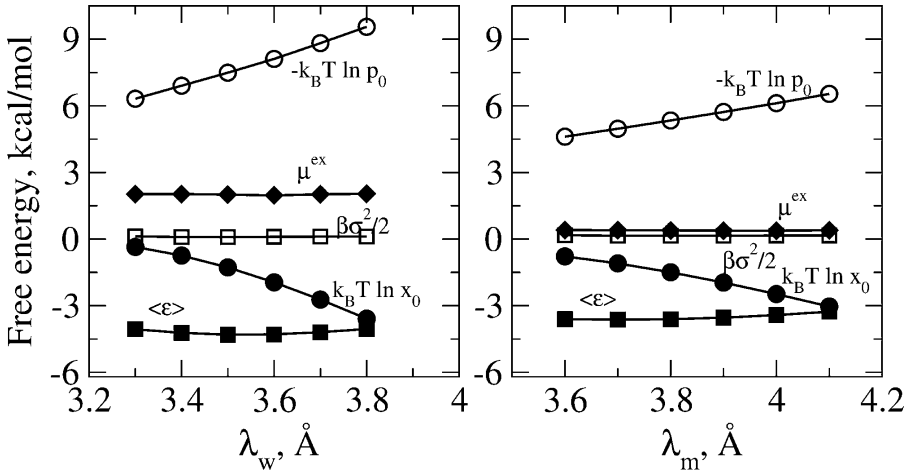

Figure 5. Left panel: QC free energy contributions to μ_s^{ex} (eq 3) for methane in water as a function of the inner-shell radius, λ_w. Right panel: QC free energy contributions to μ_s^{ex} (eq 3) for methane in methanol as a function of the inner-shell radius, $\lambda_m = \lambda_h - 0.3$ Å. Symbols: μ_s^{ex} = diamonds; $k_BT \ln x_0$ = filled circles; $-k_BT \ln p_0$ = open circles; $\langle \varepsilon \rangle$ = filled squares; $\beta\sigma^2/2$ = open squares. Lines are drawn to guide the eye. Conditional binding energy probability distributions for the different inner-shell radii are given in Figures S1 and S2 (Supporting Information).

Table 2. QC Free Energy Contributions to μ_s^{ex} (eq 3) for Methane in Aqueous Methanol Solutions as a Function of Methanol Mole Fraction[a]

mole fraction	$-k_BT \ln p_0$	$k_BT \ln x_0$	$\langle \varepsilon \rangle$	$\beta\sigma^2/2$	μ_s^{ex}
0.00	6.34	−0.36	−4.06	0.12	2.04 (2.03)
0.05	6.20	−0.45	−4.04	0.13	1.84 (1.82)
0.10	6.15	−0.52	−4.01	0.14	1.76 (1.72)
0.20	5.95	−0.62	−3.94	0.15	1.54 (1.56)
0.30	5.77	−0.70	−3.90	0.16	1.33 (1.31)
1.00	4.63	−0.78	−3.60	0.17	0.42 (0.38)

[a]Mean binding energies and fluctuation contributions are computed from conditional probability distributions in Figures 4 and S3 (Supporting Information) with λ_w = 3.3, λ_m = 3.6, and λ_h = 3.9 Å. Values of μ_s^{ex} in parentheses are calculated using histogram overlap.[25,26,57] All free energies are in kcal/mol.

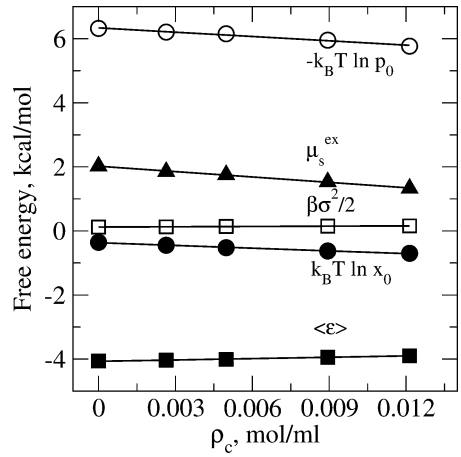

Figure 6. Methanol concentration dependence of the QC contributions to μ_s^{ex} for methane in aqueous methanol solutions evaluated using inner-shell radii of λ_w = 3.3 Å, λ_m = 3.6 Å, and λ_h = 3.9 Å. Symbols: μ_s^{ex} = filled triangles; $k_BT \ln x_0$ = filled circles; $-k_BT \ln p_0$ = open circles; $\langle \varepsilon \rangle$ = filled squares; $\beta\sigma^2/2$ = open squares. Lines are linear fits to the data. Conditional binding energy probability distribution as a function of methanol concentration (Figure S3) and error estimates associated with the Gaussian approximations for those probability distributions (Table S1) are provided in the Supporting Information.

Preferential interaction parameters computed from the slope of $\mu_s^{ex}(\rho_c)$ in Figure 6 are given in Table 3. These results are compared with Γ_{sc} derived from KB integrals and Γ_{sc} computed from the methanol concentration dependence of μ_s^{ex} computed using histogram overlap. In all cases, $\Gamma_{sc} > 0$, indicating preferential methanol−methane interactions in aqueous methanol solutions. Moreover, Γ_{sc} derived from KB theory is consistently larger in magnitude compared to Γ_{sc} derived from QC theory. In contrast, $\Gamma_{sc} \approx 0$ for a hard-sphere solute in aqueous methanol solutions over a comparable range of methanol concentrations.[38]

The individual QC contributions to Γ_{sc} are given in Table 4 as a function of the inner-shell radius for water around methane in the aqueous solution containing 10 mol % methanol. The positive contribution from the free energy of cavity formation dominates for all λ_w. Chemical association also contributes to $\Gamma_{sc} > 0$ for the smaller inner-shell volumes considered, while the mean binding energy contribution favors methane hydration, and more so for larger inner-shell volumes. The binding energy fluctuation contribution can be neglected at all λ_w. The QC contributions also compensate one another as a function of λ_w such that Γ_{sc} is essentially independent of the defined inner shell.

We note that the cavity formation free energy contribution increases in magnitude, while the chemical association contribution decreases in magnitude with increasing λ_w. Initially, the net result is an increasingly positive inner-shell contribution to Γ_{sc} as the inner shell grows in size, which reflects diminishing packing constraints on the formation of molecular clusters of methanol and water with methane in the inner shell that accordingly enhance preferential interactions between methanol and methane. This net contribution reaches a maximum at $\lambda_w \approx 3.7$ Å. The chemical association contribution also equals zero at roughly the same radius, λ_w = 3.75 Å (Table 4), which reflects the short-range nature of methane−methanol hydrophobic interactions. Thus, the inner-shell contribution to Γ_{sc} is derived solely from the free energy of cavity formation in the aqueous methanol solution alone for this inner-shell specification, and

dx.doi.org/10.1021/jp301629j | J. Phys. Chem. B 2012, 116, 6506−6513

Table 3. Methanol−Methane Preferential Interaction Parameters in Aqueous Methanol Solutions as a Function of Methanol Mole Fraction[a]

methanol mole fraction	$\rho_c \times 10^3$ (mol/ml)	Γ_{sc} (eq 6)	Γ_{sc} (eq 5)	Γ_{sc} (eq 4)
0.05	2.64	0.32	0.25	0.25
0.10	4.98	0.61	0.47	0.46
0.20	8.94	1.22	0.84	0.83
0.30	12.14	1.48	1.14	1.13

[a]Γ_{sc} from KB theory (eq 6) is computed using a cutoff radius of R = 6.0 Å to evaluate the KB integrals (eq 7) from the methane−water and methane−methanol radial distribution functions in Figures 2 and 3. Spatial locations of water and methanol molecules around the solute are defined with respect to their center-of-mass coordinates.[45] Γ_{sc} from QC theory (eq 5) is computed from the slope of $\mu_s^{ex}(\rho_c)$ in Figure 6. Γ_{sc} is also calculated using eq 4 with the μ_s^{ex} in Table 2 derived from the histogram overlap method.[25,26,57] Units for Γ_{sc} are number of methanol molecules/methane molecule.

Table 4. QC Contributions to the Methane−Methanol Preferential Interaction Parameter Γ_{sc} for 10 mol % Methanol/Water Solution as a Function of the Inner-Shell Radius for Water, λ_w[a]

λ_w (Å)	$\left(\frac{\partial \ln p_0}{\partial \ln \rho_c}\right)$	$-\left(\frac{\partial \ln x_0}{\partial \ln \rho_c}\right)$	$-\left(\frac{\partial \beta\langle\varepsilon\rangle}{\partial \ln \rho_c}\right)$	$-\left(\frac{\partial \beta^2\sigma^2/2}{\partial \ln \rho_c}\right)$	Γ_{sc}
3.3	+0.38	+0.24	−0.12	−0.03	+0.47
3.4	+0.45	+0.23	−0.17	−0.03	+0.48
3.5	+0.52	+0.20	−0.21	−0.03	+0.48
3.6	+0.61	+0.14	−0.24	−0.03	+0.48
3.7	+0.72	+0.05	−0.26	−0.02	+0.49
3.8	+0.79	−0.05	−0.24	−0.01	+0.49

[a]The corresponding radii for the methyl and hydroxyl groups of methanol are $\lambda_m = \lambda_w + 0.3$ Å and $\lambda_h = \lambda_w + 0.6$ Å, respectively. Units for Γ_{sc} are the number of methanol molecules/methane molecule.

$$\Gamma_{sc}(\lambda_w = 3.7\text{Å}) \approx \rho_c\left(\frac{\partial \ln p_0}{\partial \rho_c}\right)_{T,P,\rho_s} - \rho_c\left(\frac{\partial \beta\langle\varepsilon\rangle}{\partial \rho_c}\right)_{T,P,\rho_s} \quad (8)$$

The solute contributes through the defined inner shell/cavity size and shape, as discussed below, and its intermolecular interactions with the outer-shell solvent. Since close contact, repulsive interactions between the solute and solvent molecules have been removed from this outer-shell contribution, these interactions involve only nonlocal (long-range) attractions. The expectation is that this contribution can be reasonably estimated using approximate (mean field) models. The molecular details of cosolvent preferential interactions with the solute are derived from molecular packing constraints of the cosolvent in the aqueous methanol solution alone through the free energy of cavity formation as a function of methanol concentration. This counterintuitive result is not surprising given that the free energy of cavity formation in water alone plays a central role in the molecular theory of hydrophobicity.[54−56,62] The extension here to preferential hydrophobic interactions in aqueous solutions, however, requires the specification of a unique inner shell for which there is no chemical association contribution to Γ_{sc}. Although eq 8 was obtained for the 10% methanol/water solution specifically, this unique inner-shell specification is found to be insensitive to the methanol concentration over the entire range of concentrations considered.

Equation 8 suggests that cosolvent effects on hydrophobic driving forces for molecular recognition and self-assembly can be correlated with the cosolvent concentration dependence of the air−aqueous solution interfacial tension. Indeed, such correlations have been found but are generally much stronger for added salts compared to polar or nonpolar cosolvents.[63−69] It also follows that these cosolvent effects will be correlated with cosolvent molecular size. For macromolecular cosolvents, or smaller amphiphilic cosolvents that self-associate to form larger molecular clusters in aqueous solution, size-dependent cosolvent effects are explained in terms of macromolecular crowding or the steric exclusion of cosolvent from the local domain around the solute, which create depletion forces.[2,8,70,71] Molecular size-dependent cosolvent effects have also been observed for small-molecule cosolvents not known to self-associate into larger clusters. For example, the stabilizing effect of added low-molecular-weight polyols and sugars on peptide folding driven by hydrophobic interactions is found to be cosolvent-size-dependent but is also accompanied by a decrease in the favorable entropy of folding, which cannot be explained by a steric exclusion or crowding mechanism.[72] Equation 8 can provide an alternative explanation by considering peptide site-specific cosolvent hydrophobic preferential interactions for the different polyols and sugars.

The inner-shell volumes considered here by definition include only a fraction of the first solvation shell of methane. At λ_w = 3.7 Å, the compensating contribution from the mean binding energy is also significant (Table 4), which emphasizes the importance of including the outer-shell contribution in evaluating Γ_{sc}. We note that this outer-shell QC contribution does not simply require material balances for water and the cosolvent to be satisfied across different domains in the entire, closed simulation system, which has been shown to improve convergence in evaluating KB integrals.[20,21,23] Instead, the outer-shell contribution provides thermodynamic preferences for certain molecular clusters that can form within the defined inner shell, and as such is essential for accurately assessing cosolvent preferential interactions. A comparable thermodynamic weighting is carried out implicitly in evaluating the KB integrals by normalizing local water and cosolvent densities using effective bulk solution densities. This normalization, however, requires much larger simulation systems that permit the local domain around the solute to include multiple solvation shells.[45]

V. CONCLUSIONS

The QC/PDT analysis presented here quantitatively captures the favorable solvation of methane in aqueous methanol solutions in terms of important local and nonlocal free energy contributions to cosolvent hydrophobic preferential interactions with the solute. Local contributions are derived from the free energy of forming molecular clusters of water and cosolvent with the solute inside a defined inner shell around the solute, and from the free energy of forming a cavity the size and shape of this inner shell in the aqueous cosolvent solution alone. Nonlocal contributions arise from solute interactions with water and cosolvent molecules outside the defined inner shell under the condition that no solvent molecules occupy the inner shell.

In addition, a unique inner shell around the solute can be defined, such that methane−methanol preferential interactions are determined from the methanol concentration dependence of the free energy of cavity formation in the aqueous methanol

dx.doi.org/10.1021/jp301629j | J. Phys. Chem. B 2012, 116, 6506−6513

solution alone, and the mean binding energy of methane with solvent outside the defined inner shell. Thus, the molecular details of these preferential interactions are described by cavity statistics for the aqueous cosolvent solution in the absence of the solute, once the size and shape of this unique inner shell are defined. An accurate treatment of the mean binding energy of methane with outer-shell solvent may be obtained by applying approximate solution thermodynamic models, rather than resorting to detailed calculations of intermolecular interactions from simulation trajectories. The central role cavity statistics plays in this QC/PDT analysis highlights the importance of molecular packing constraints in characterizing cosolvent hydrophobic preferential interactions, and suggests that excluded volume interactions beyond steric exclusion (macromolecular crowding) contribute to these preferential interactions. Nonlocal solute−solvent interactions also play an essential role in the analysis by ensuring the preferential interactions are independent of the distinction between local and nonlocal solute interactions with the solvent that is made by defining an inner shell around the solute.

Finally, the defined inner shell around the solute is significantly smaller than the local domain required to reliably evaluate preferential interactions from KB integrals, which require the normalization of the solute−solvent molecular distribution functions. Thus, higher spatial resolution can be achieved in describing local preferential interactions, which opens up the possibility of evaluating site-specific preferential interactions across the solvent accessible surface of complex, chemically heterogeneous macromolecular solutes using this QC/PDT approach.

■ ASSOCIATED CONTENT

Supporting Information

Tables, figures, and text describing error estimation of Gaussian approximation for the outer-shell contribution to the solute excess chemical potential. This material is available free of charge via the Internet at http://pubs.acs.org.

■ AUTHOR INFORMATION

Notes

The authors declare no competing financial interest.

■ ACKNOWLEDGMENTS

Financial support from the National Science Foundation (BES-0555281), the Department of Energy (DE-FG02-04ER25626), and the American Chemical Society Petroleum Research Foundation is gratefully acknowledged. We also thank Lawrence Pratt (Tulane University) for numerous stimulating and helpful discussions.

■ REFERENCES

(1) Timasheff, S. N. Control of Protein Stability and Reactions by Weakly Interacting Cosolvents: The Simplicity of the Complicated. *Adv. Protein Chem.* **1998**, *51*, 355−432.

(2) Parsegian, V. A.; Rand, R. P.; Rau, D. C. Osmotic stress, crowding, preferential hydration, and binding: A comparison of perspectives. *Proc. Natl. Acad. Sci. U.S.A.* **2000**, *97*, 3987−3992.

(3) Roesgen, J.; Pettitt, B. M.; Bolen, D. W. Protein Folding, Stability, and Solvation Structure in Osmolyte Solutions. *Biophys. J.* **2005**, *89*, 2988−2997.

(4) Shukla, D.; Schneider, C. P.; Trout, B. L. Molecular level insight into intra-solvent interaction effects on protein stability and aggregation. *Adv. Drug Delivery Rev.* **2011**, *63*, 1074−1085.

(5) Kamerzell, T. J.; Esfandiary, R.; Joshi, S. B.; Middaugh, C. R.; Volkin, D. B. Protein-excipient interactions: Mechanisms and biophysical characterization applied to protein formulation development. *Adv. Drug Delivery Rev.* **2011**, *63*, 1118−1159.

(6) Berger, B. W.; Gendron, C. M.; Lenhoff, A. M.; Kaler, E. W. Effects of additives on surfactant phase behavior relevant to bacteriorhodopsin crystallization. *Protein Sci.* **2006**, *15*, 2682−2696.

(7) Dumetz, A. C.; Chockla, A. M.; Kaler, E. W.; Lenhoff, A. M. Comparative Effects of Salt, Organic, and Polymer Precipitants on Protein Phase Behavior and Implications for Vapor Diffusion. *Cryst. Growth Des.* **2009**, *9*, 682−691.

(8) Shukla, D.; Trout, B. L. Interaction of Arginine with Proteins and the Mechanism by Which It Inhibits Aggregation. *J. Phys. Chem B* **2010**, *114*, 13426−13438.

(9) Ignatova, Z.; Gierasch, L. M. Inhibition of protein aggregation in vitro and in vivo by a natural osmoprotectant. *Proc. Natl. Acad. Sci. U.S.A.* **2006**, *103*, 13357−13361.

(10) Evers, F.; Steitz, R.; Tolan, M.; Czeslik, C. Reduced Protein Adsorption by Osmolytes. *Langmuir* **2011**, *27*, 6995−7001.

(11) Mollmann, S. H.; Elofsson, U.; Bukrinsky, J. T.; Frokjaer, S. Displacement of adsorbed insulin by Tween 80 monitored using total internal reflection fluorescence and ellopsometry. *Pharm. Res.* **2005**, *22*, 1931−1941.

(12) Yang, D. S.; Yip, C. M.; Huang, T. H. J.; Chakrabartty, A.; Fraser, P. E. Manipulating the amyloid-beta aggregation pathway with chemical chaperones. *J. Biol. Chem.* **1999**, *274*, 32970−32974.

(13) Nayak, A.; Lee, C.-C.; McRae, G. J.; Belfort, G. Osmolyte Controlled Fibrillation Kinetics of Insulin: New Insight into Fibrillation Using the Preferential Exclusion Principle. *Biotechnol. Prog.* **2009**, *25*, 1508−1514.

(14) Reza, K.; Hosnieh, S.; Mojtaba, A. Study of Cosolvent-Induced alpha-Chymotrypsin Fibrillogenesis: Does Protein Surface Hydrophobicity Trigger Early Stages of Aggregation Reaction? *Protein J.* **2009**, *28*, 349−361.

(15) Gekko, K.; Timasheff, S. N. Mechanism of Protein Stabilization by Glycerol - Preferential Hydration in Glycerol-Water Mixtures. *Biochemistry* **1981**, *20*, 4667−4676.

(16) Liu, W.; Bratko, D.; Prausnitz, J. M.; Blanch, H. W. Effect of alcohols on aqueous lysozyme-lysozyme interactions from static light scattering measurements. *Biophys. Chem.* **2004**, *107*, 289−298.

(17) Sousa, R. Use of Glycerol, Polyols and Other Protein Structure Stabilizing Agents in Protein Crystallization. *Acta Crystallogr., Sect. D* **1995**, *51*, 271−277.

(18) Gosavi, R. A.; Mueser, T. C.; Schall, C. A. Optimization of Buffer Solutions for Protein Crystallization. *Acta Crystallogr., Sect. D* **2008**, *64*, 506−514.

(19) Abbas, S. A.; Sharma, V. K.; Patapoff, T. W.; Kalonia, D. S. Solubilities and Transfer Free Energies of Hydrophobic Amino Acids in Polyol Solutions: Importance of the Hydrophobicity of Polyols. *J. Pharm. Sci.* **2011**, *100*, 3096−3104.

(20) Baynes, B. M.; Trout, B. L. Proteins in Mixed Solvents: A Molecular-Level Perspective. *J. Phys. Chem. B* **2003**, *107*, 14058−14067.

(21) Kang, M.; Smith, P. E. Preferential Interaction Parameters in Biological Systems by Kirkwood-Buff Theory and Computer Simulation. *Fluid Phase Equilib.* **2007**, 14−19.

(22) Smolin, N.; Winter, R. Effect of temperature, pressure, and cosolvents on structural and dynamic properties of the hydration shell of SNase: A molecular dynamics computer simulation study. *J. Phys. Chem. B* **2008**, *112*, 997−1006.

(23) Shukla, D.; Shinde, C.; Trout., B. L. Molecular Computations of Preferential Interaction Coefficients of Proteins. *J. Phys. Chem. B* **2009**, *113* (37), 12546−12554.

(24) Paulaitis, M. E.; Pratt, L. R. Hydration Theory for Molecular Biophysics. *Adv. Protein Chem.* **2002**, *62*, 283−310.

(25) Pratt, L. R.; Asthagiri, D. Potential distribution methods and free energy models of molecular solutions. In *Free energy calculations: Theory and applications in chemistry and biology*; Chipot, C., Pohorille,

A., Eds.; Springer Series in Chemical Physics, Vol. *86*; Springer: New York, 2007; Chapter 9, pp 323−351.
(26) Beck, T. L.; Paulaitis, M. E.; Pratt, L. R. *The potential distribution theorem and models of molecular solutions*; Cambridge University Press: Cambridge, U.K., 2006.
(27) Ashbaugh, H. S.; Asthagiri, D.; Pratt, L. R.; Rempe, S. B. Hydration of Krypton and Consideration of Clatharate Models of Hdrophobic Effects from the Perspective of Quasi-chemical Theory. *Biophys. Chem.* **2003**, *105*, 323−338.
(28) Asthagiri, D.; Ashbaugh, H. S.; Priyatinski, A.; Paulaitis, M. E.; Pratt, L. R. Non-van der Waals Treatment of the Hydrophobic Solubilities of CF_4. *J. Am. Chem. Soc.* **2007**, *129*, 10133−10140.
(29) Asthagiri, D.; Merchant, S.; Pratt, L. R. Role of Attractive Methane-Water Interactions in the Potential of Mean Force between Methane Molecules in Water. *J. Chem. Phys.* **2008**, *128*, 244512-1−244512-7.
(30) Widom, B. Some topics in the theory of fluids. *J. Chem. Phys.* **1963**, *39*, 2808−2812.
(31) Widom, B. Potential-distribution theory and the statistical mechanics of fluids. *J. Phys. Chem.* **1982**, *86*, 869−872.
(32) Shah, J. K.; Asthagiri, D.; Pratt, L. R.; Paulaitis, M. E. Balancing Local Order and Long-ranged Interactions in the Molecular Theory of Liquid Water. *J. Chem. Phys.* **2007**, *127*, 144508−1−144508−7.
(33) Utiramerur, S.; Paulaitis, M. E. Cooperative hydrophobic/hydrophilic interactions in the hydration of dimethyl ether. *J. Chem. Phys.* **2010**, *132*, 155102-1−155102-9.
(34) Asthagiri, D.; Dixit, P. D.; Merchant, S.; Paulaitis, M. E.; Rempe, S. B.; Pratt, L. R.; Varma, S. Ion selectivity from local configurations of ligands. *Chem. Phys. Lett.* **2010**, *485*, 1−7.
(35) Merchant, S.; Dixit, P. D.; Dean, K. R.; Asthagiri, D. Ion-water, bulk medium effects, and ion hydration. *J. Chem. Phys.* **2011**, *135*, 155102-1−155102-8.
(36) Kirkwood, J. G.; Buff, F. P. The Statistical Mechanical Theory of Solutions. I. *J. Chem. Phys.* **1951**, *19*, 774−777.
(37) Smith, P. E. Chemical Potential Derivatives and Preferential Interaction Parameters in Biological Systems from Kirkwood-Buff Theory. *Biophys. J.* **2006**, *91*, 849−856.
(38) Shah, P. K.; Roberts, C. J. Molecular Solvation in Water-Methanol and Water-Sorbitol Mixtures: The Roles of Preferential Hydration, Hydrophobicity, and the Equation of State. *J. Phys. Chem. B* **2007**, *111*, 4467−4476.
(39) Chitra, R.; Smith, P. E. Preferential Interactions of Cosolvents with Hydrophobic Solutes. *J. Phys. Chem. B* **2001**, *105*, 11513−11522.
(40) Smith, P. E. Computer Simulation of Cosolvent Effects on Hydrophobic Hydration. *J. Phys. Chem. B* **1999**, *103*, 525−534.
(41) Kokubo, H.; Pettitt, B. M. Preferential solvation in urea solutions at different concentrations: Properties from simulation studies. *J. Phys. Chem. B* **2007**, *111*, 5233−5242.
(42) Lockwood, D. M.; Rossky, P. J. Evaluation of Functional Group Contribution to Excess Volumetric Properties of Solvated Molecules. *J. Phys. Chem. B* **1999**, *103*, 1982−1990.
(43) Lockwood, D. M.; Rossky, P. J. Functional Group Contributions to Partial Molar Compressibilities of Alcohols in Water. *J. Phys. Chem. B* **2000**, *104*, 4210−4217.
(44) Sangwai, A. V.; Ashbaugh, H. S. Aqueous Partial Molar Volumes from Simulation and Individual Group Contributions. *Ind. Eng. Chem. Res.* **2008**, *47*, 5169−5174.
(45) Hamsa Priya, M.; Ashbaugh, H. S.; Paulaitis, M. E. Cosolvent Preferential Molecular Interactions in Aqueous Solutions. *J. Phys. Chem. B* **2011**, *115*, 13633−13642.
(46) Kalé, L.; Skeel, R.; Bhandarkar, M.; Brunner, R.; Kraweta, N. G. N.; Phillips, J.; Shinozaki, A.; Varadarajan, K.; Schulten, K. NAMD2: Greater Scalability for Parallel Molecular Dynamics. *J. Comput. Phys.* **1999**, *151*, 283−312.
(47) Jorgensen, W. L.; Madura, J. D.; Swenson, C. J. Optimized Intermolecular Potential Functions for Liquid Hydrocarbons. *J. Am. Chem. Soc.* **1984**, *106*, 6638−6646.
(48) Jorgensen, W. L. Optimized Intermolecular Potential Function for Liquid Alcohols. *J. Phys. Chem.* **1986**, *90*, 1276−1284.
(49) Jorgensen, W. L.; Chandrasekhar, J.; Madura, J. D.; Impey, R. W.; Klein, M. L. Comparison of Simple Potential Functions for Simulating Liquid Water. *J. Chem. Phys.* **1983**, *79*, 926−935.
(50) Martyna, G. J.; Tobias, D. J.; Klein, M. L. Constant Pressure Molecular Dynamics Algorithms. *J. Chem. Phys.* **1994**, *101*, 4177−4189.
(51) Feller, S. E.; Zhang, Y.; Pastor, R. W. Constant Pressure Molecular Dynamics Simulations: The Langevin Piston Method. *J. Chem. Phys.* **1995**, *103*, 4613−4621.
(52) Darden, T.; York, D.; Pedersen, L. Particle Mesh Ewald: An N log(N) Method for Ewald Sums in Large Systems. *J. Chem. Phys.* **1993**, *98*, 10089−10092.
(53) Ryckaert, J. P.; Ciccotti, G.; Berendsen, H. J. C. Numerical Integration of the Cartesian Equations of Motion of a System with Constraints: Molecular Dynamics of n-Alkanes. *J. Comput. Phys.* **1977**, *23*, 327−341.
(54) Hummer, G.; Garde, S.; Garcia, A. E; Paulaitis, M. E.; Pratt, L. R. Hydrophobic Effects on a Molecular Scale. *J. Phys. Chem. B* **1998**, *102*, 10469−10481.
(55) Pratt, L. R.; Pohorille, A. Theory of Hydrophobicity: Transient Cavities in Molecular Liquids. *Proc. Natl. Acad. Sci. U.S.A.* **1992**, *89*, 2995−2999.
(56) Pohorille, A.; Pratt, L. R. Cavities in Molecular Liquids and the Theory of Hydrophobic Solubilities. *J. Am. Chem. Soc.* **1990**, *112*, 5066−5074.
(57) Bennett, C. H. Efficient estimation of free energy differences from Monte Carlo data. *J. Comput. Phys.* **1976**, *22*, 245−268.
(58) Konard, O.; Lankau, T. Solubility of Methane in Water: The Significance of the Methane-Water Interaction Potential. *J. Phys. Chem. B* **2005**, *109*, 23596−23604.
(59) Yaacobi, M.; Ben-Naim, A. Solvophobic Interaction. *J. Phys. Chem.* **1974**, *78* (2), 175−178.
(60) Ben-Naim, A.; Marcus, Y. Solvation thermodynamics of nonionic solutes. *J. Chem. Phys.* **1984**, *81*, 2016−2027.
(61) Wescott, J. T.; Fisher, L. R.; Hanna, S. J. Use of thermodynamic integration to calculate the hydration free energies of n-alkanes. *J. Chem. Phys.* **2002**, *116*, 2361−2369.
(62) Hummer, G.; Garde, S.; Garcia, A. E.; Pohorille, A.; Pratt, L. R. An information theory model of hydrophobic interactions. *Proc. Natl. Acad. Sci. U.S.A.* **1996**, *93* (17), 8951−8955.
(63) Kita, Y.; Arakawa, T.; Lin, T.-Y.; Timasheff, S. N. Contribution of the Surface Free Energy Perturbation to Protein-Solvent Interactions. *Biochemistry* **1994**, *33*, 15178−15189.
(64) Cioci, F.; Lavecchia, R.; Marrelli, L. Perturbation of Surface-Tension of Water by Polyhydric Additives - Effect of Glucose-Oxidase Stability. *Biocatalysis* **1994**, *10*, 137−147.
(65) Cioci, F. Effect of surface tension on the stability of heat-stressed proteins: A molecular thermodynamic interpretation. *J. Phys. Chem.* **1996**, *100*, 17400−17405.
(66) Lin, T. Y.; Timasheff, S. N. On the role of surface tension in the stabilization of globular proteins. *Protein Sci.* **1996**, *5*, 372−381.
(67) Ghosh, T.; Kalra, A.; Garde, S. On the salt-induced stabilization of pair and many-body hydrophobic interactions. *J. Phys. Chem. B* **2005**, *109*, 642−651.
(68) Harries, D.; Rau, D. C.; Parsegian, V. A. Solutes probe hydration in specific association of cyclodextrin and adamantane. *J. Am. Chem. Soc.* **2005**, *127*, 2184−2190.
(69) Chanasattru, W.; Decker, E. A.; McClements, D. J. Impact of cosolvents (polyols) on globular protein functionality: Ultrasonic velocity, density, surface tension and solubility study. *Food Hydrocolloids* **2008**, *22*, 1475−1484.
(70) Zimmerman, S. B.; Minton, A. P. Macromolecular Crowding - Biochemical, Biophysical, and Physiological Consequences. *Annu. Rev. Biophys. Biomol. Struct.* **1993**, *22*, 27−65.
(71) Ellis, R. J.; Minton, A. P. Protein aggregation in crowded environments. *Biol. Chem.* **2006**, *387*, 485−497.
(72) Politi, R.; Harries, D. Enthalpically driven peptide stabilization by protective osmolytes. *Chem. Commun.* **2010**, *46*, 6449−6451.